J. Indian Inst. Sci., 63 (A), Jan. 1981, Pp. 21-38

Aeroacoustic analysis of mufflers with flow reversals

V. B. PANICKER* AND M. L. MUNJAL
Department of Mechanical Engineering, Indian Institute of Science, Bangalore 560 012, India.

Abstract

Mufflers with reversals of the direction of flow of exhaust gases are analysed. The transfer matrices relating the aeroacoustic variables across flow reversing elements are derived. The head loss factors at these elements required in the energy equations are determined experimentally. The noise reduction spectra of mufflers with flow reversals are determined experimentally and compared with the predicted results. The predicted results of noise reduction characteristics of experimental mufflers agree very well with the measured values. That corroborates the validity of the derivation procedure and exactness of the transfer matrices, so obtained.

Key words : Exhaust mufflers, aero flow acoustics, engine noise contral.

1. Introduction

The theoretical analysis of exhaust mufflers has been restricted to the straight-through types till recent times. Of late, in several commercial designs of mufflers, reversals of the direction of mean flow of exhaust gases have been introduced. These designs have shown an overall improvement in the attenuation characteristics over those of the straight-through types. Consequently, mufflers with flow reversals have become popular in commercial use. There is a move in Europe in favour of adoption of reversed flow mufflers in place of the absorbing types used at present[1].

Reversed flow mufflers have many variations as shown in fig. 1. The direction of flow of exhaust gases is reversed once or several times inside the muffler and elements such as Helmholtz resonators, concentric resonators and reversing end chambers are connected at intervals. In addition, controlled cross flow among different tubes is often allowed which produces attenuation perhaps by virtue of the fact that the sound waves can progress by alternate paths of different lengths resulting in interference. Reversed flow mufflers, however, generally increase the back pressure and consequently the engine performance suffers.

* Presently with the Department of Mechanical Engineering, N.S.S. College of Engineering, Palghat 678 008, Kerala, India.

(a) Muffler with single flow reversal

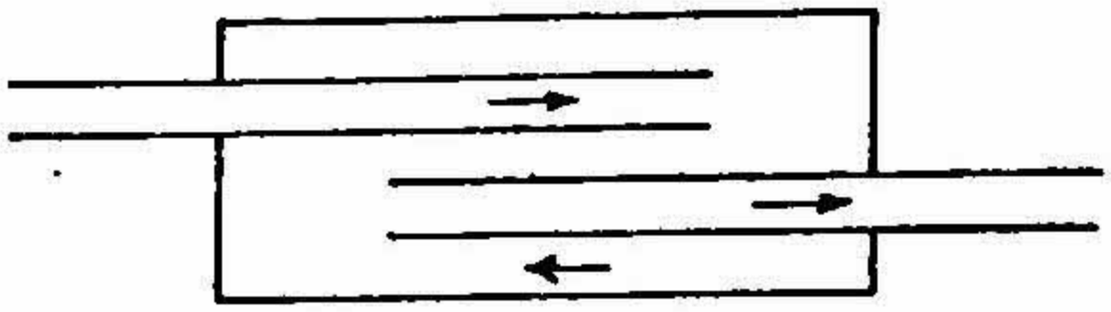

(b) Muffler with two flow reversals

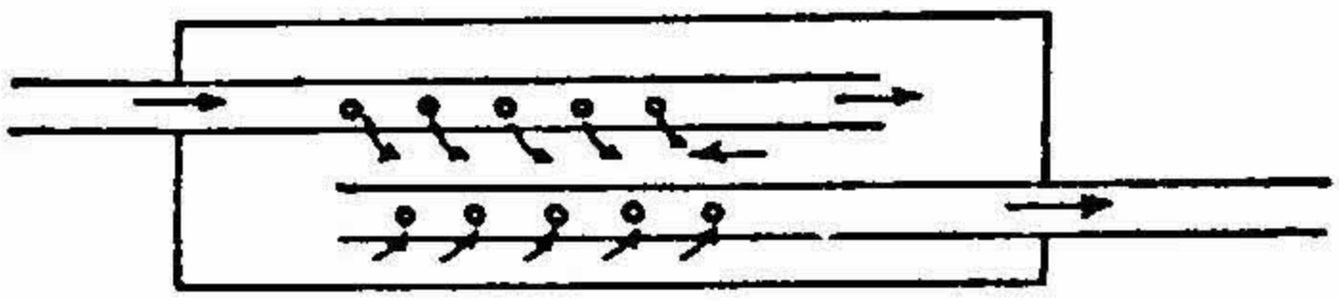

(c) Reversed-flow muffler with restricted cross flow

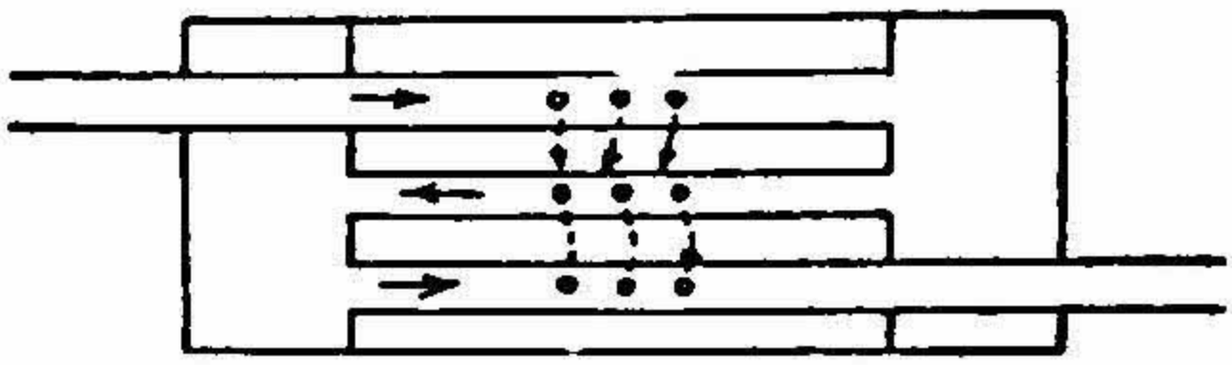

(d) Muffler with three flow reversals and side resonator

FIG. 1. Variations of reversed flow mufflers.

2. Review of previous work

On account of the difficulty experienced in the formulation of explicit (non-iterative) mathematical models characterising the acoustic behaviour of muffler elements with cross flow and multiple flow paths[2–4], the development in the analysis of such mufflers has been rather slow. Two types of flow reversing elements have been considered in this paper. They are :

(i) Reversal-contraction, and

(ii) Reversal-expansion.

Figure 2 shows these elements indicating the locations of reference points for the purpose of derivation of the relations of the convective or aeroacoustic state variables[5]. Making use of the equations of mass continuity, momentum balance and energy relations with and without acoustic perturbations, Munjal and Bapat[6] derived transfer matrices for both the flow reversing elements. Assuming

$$M^2 \sim N^2 \sim NM \ll 1$$

where

M—flow Mach number,

$$N\text{—area ratio} = \frac{\text{Area of inner tube}}{\text{Annular area of the outer tube}}$$

they obtained the following transfer matrix relations

(i) *Reversal-contraction*

$$\begin{bmatrix} p_{e,2} \\ v_{e,2} \end{bmatrix} = \begin{bmatrix} 1 & 0 \\ \frac{1}{Z_2} & 1 \end{bmatrix} \begin{bmatrix} p_{e,1} \\ v_{e,1} \end{bmatrix} \tag{1}$$

where p_e and v_e are the aeroacoustic pressure and mass velocity respectively[5], related linearly with classical acoustic variables p and v

$Z_2 = -iY_2 \cot kl_2$

$i = \sqrt{-1}$

$Y_2 = c/S_2$

c = acoustic wave velocity

S_2 = area of cross-section of the reversing end chamber

$k = \omega/c$

$\omega = 2\pi f$

f = frequency, Hz and

l_2 = length of the flow reversing end chamber.

(ii) *Reversal-expansion*

The corresponding transfer matrix relation obtained in ref. 6 is

$$\begin{bmatrix} p_{e,2} \\ v_{e,2} \end{bmatrix} = \frac{1}{1+N-NA(1+a_e)} \begin{bmatrix} 1+N-A(N-a_e) & a_e M_2 Y_2 \\ \frac{1+N}{Z_2} & 1 \end{bmatrix} \begin{bmatrix} p_{e,1} \\ v_{e,1} \end{bmatrix} \tag{2}$$

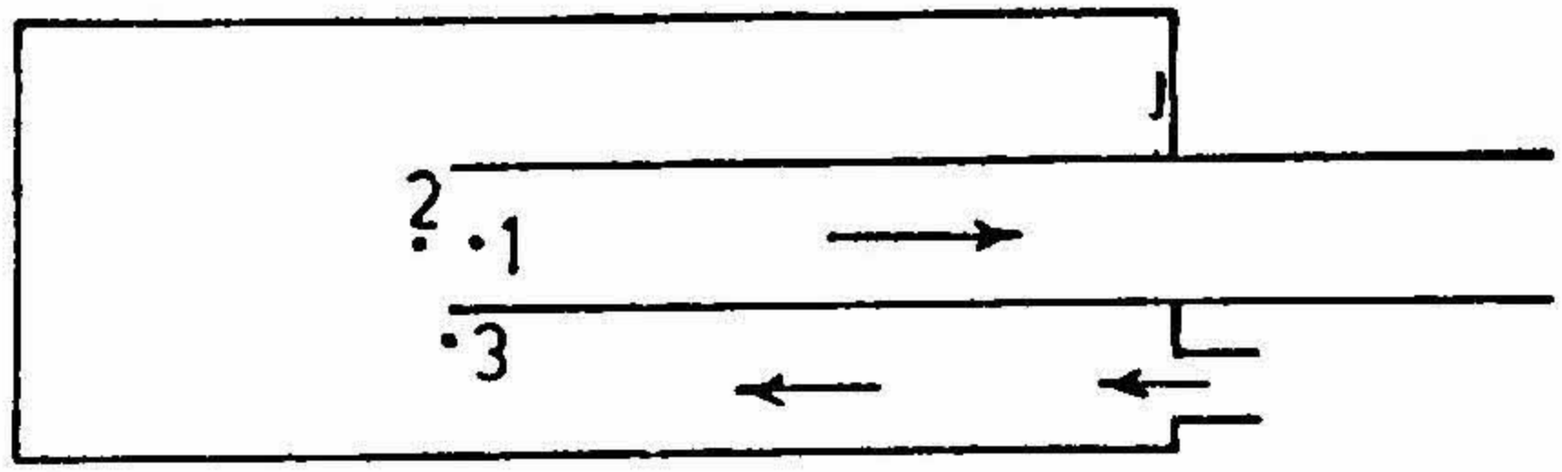

(a) Flow reversal - cum - contraction

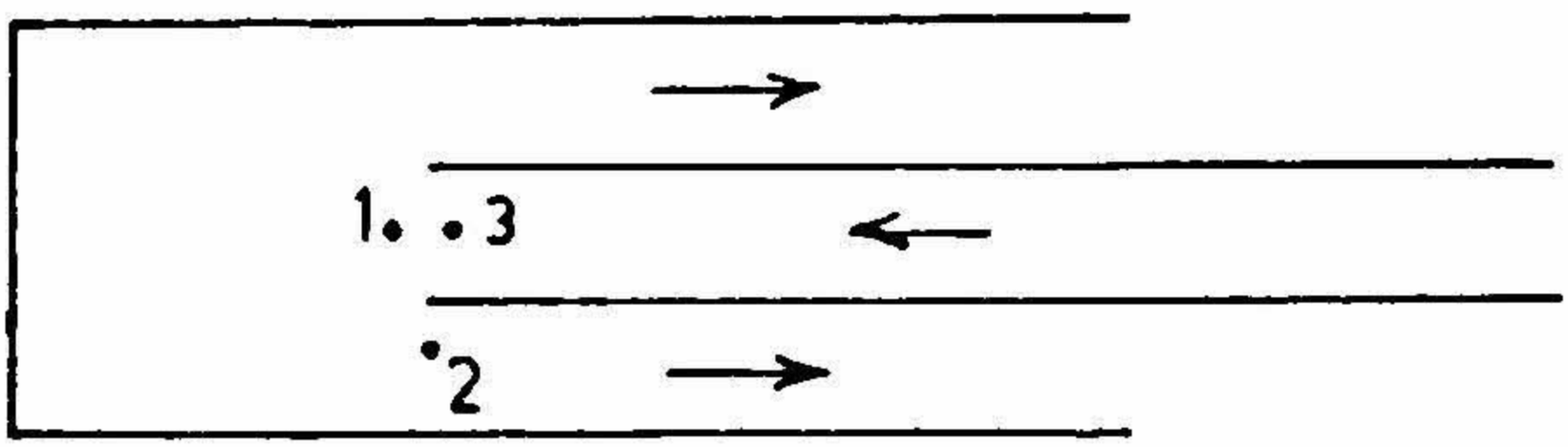

(b) Flow reversal - cum - expansion

FIG. 2. Flow reversing elements.

where

$$N = S_3/S_1$$

$$A = \frac{M_3 Y_3}{Z_2}$$

and a_e is the head loss coefficient expressed as the ratio of the loss of total pressure to the dynamic head in the smaller tube at reversal-*cum*-expansion.

Munjal and Bapat[6] suggested that the value of a_e might be between 2 and 3 which was, however, not supported by experimental evidence. Thawani[7] adopting this value, predicted the noise reduction characteristics of experimental mufflers and reported a fairly satisfactory agreement between the predicted and measured values.

The transfer matrix for flow reversal-*cum*-contraction given by eqn. (1) presumes that the pressure in the end chamber (at point 2 in fig. 2) is equal to the total pressure upstream (at point 3) and that the latter is equal to the total pressure downstream

(at point 1). In practice, however, some losses occur in the total pressure across the area discontinuity on account of the change in the direction of flow and a sudden change in the cross-sectional area. In terms of the aeroacoustic pressure (which represent perturbations on total pressures[5]) the above statement means

$$p_{a_1} < p_{a_3}. \tag{3}$$

Further, it can be shown from the momentum equation that

$$p_2 > p_{a_3}. \tag{4}$$

In the present paper, transfer matrices are derived incorporating the losses in total pressure across the flow reversing elements. The accuracy of the new transfer matrices is verified by comparing the theoretical noise reduction of certain test mufflers with experimental results. It may be seen that the simplification $N^2 \sim NM \ll 1$, made in refs. 2, 3 may not be valid always. So this has also been avoided here.

3. Transfer matrices for flow reversal elements

3.1. *Flow reversal with contraction*

Figure 2 (*a*) indicates the locations of points 1 and 3 across which the aeroacoustic variables p_a and v_a are to be related by a transfer matrix. While the condition upstream of the area change can be considered to be isentropic, that downstream is accompanied by an entropy change. Mungur and Gladwell[8] have suggested that the entropy fluctuation at the downstream section is given by

$$s' = -\frac{\delta}{\rho_0 T(\gamma - 1)} \tag{5}$$

where

δ is a dissipation parameter which depends on viscosity and heat conduction

ρ_0 = the density of the unperturbed medium,

T = temperature, degrees Kelvin,

γ = the ratio of specific heats.

Accordingly,

$$\rho_3 = \frac{p_3}{c^2} \tag{6}$$

and

$$\rho_1 = \frac{p_1 + \delta}{c^2} \tag{7}$$

where ρ is the density perturbation.

As explained in ref. 9, the relations governing aeroacoustic variables across the junction are :

(*a*) *Energy relations*

$$p_{c,3} = p_{c,1} + a_c M_1 Y_1 v_1 \simeq P_{c,1} + a_c M_1 Y_1 v_{c,1} \tag{8}$$

$$= p_{c,1} - \frac{\delta}{(\gamma - 1)} \tag{9}$$

where a_c is the head loss factor expressed as the ratio of the loss in total pressure across the reversal-*cum*-contraction element, to the dynamic head in the smaller tube.

(*b*) *Mass continuity*

$$v_{c,3} = v_{c,1} + v_2 + \delta \frac{M_1}{Y_1} \tag{10}$$

where

$$v_2 = p_2 / Z_2 \tag{11}$$

and

Z_2 = the equivalent impedance at section 2 of the end chamber which is given by

$$Z_2 = -iY_2 \cot kl_2.$$

(*c*) *Momentum balance*

$$p_{c,3} + M_3 Y_3 v_{c,3} + N(p_{c,1} + M_1 Y_1 v_{c,1}) + \delta N M_1^2 = N_{23} p_2 \tag{12}$$

where

$$N = S_1/S_3 = Y_3/Y_1 = M_3/M_1 \tag{13}$$

and

$$N_{23} = S_2/S_3. \tag{14}$$

It may be noted that on account of the finite thickness of the inner tube,

$$N_{23} \neq 1 + N \tag{15}$$

as was assumed in refs. 6, 7.

Solving eqns. (8), (9), (10), (11) and (12) simultaneously one gets

$$v_{c,3} = \frac{1}{N_{23} - AN^2} \left[\frac{1 + N}{Z_2} p_{c,1} + (N_{23} + A(N + a_c)) v_{c,1} \right] \tag{16}$$

where

$$A = \frac{M_1 Y_1}{Z_2}. \tag{17}$$

Equations (8) and (16) can be combined to yield the required transfer matrix relation

$$\begin{bmatrix} p_{e,2} \\ v_{e,2} \end{bmatrix} = \begin{bmatrix} 1 & a_e M_1 Y_1 \\ \dfrac{1+N}{Z_2(N_{22}-AN^2)} & \dfrac{N_{22}+A(N+a_e)}{N_{22}-AN^2} \end{bmatrix} \begin{bmatrix} p_{e,1} \\ v_{e,1} \end{bmatrix}. \tag{18}$$

If $N^2 \sim AN^2 \ll 1$, then $N_{22} \simeq 1 + N$ and hence, the transfer matrix can be written as

$$\begin{bmatrix} 1 & a_e M_1 Y_1 \\ \dfrac{1}{Z_2} & 1 + \dfrac{A(N+a_e)}{1+N} \end{bmatrix}. \tag{19}$$

If the flow reversal is made ideally smooth, then $a_e \to 0$ and the matrix (19) would become

$$\begin{bmatrix} 1 & 0 \\ \dfrac{1}{Z_2} & 1 + AN \end{bmatrix}. \tag{20}$$

Comparing the matrix (20) with (1), it is clear that the extra term 'AN' in the second-row second-column element is the result of the pressure in the end chamber not being equal to the stagnation pressure upstream or downstream of the area discontinuity. The value of a_e has been experimentally determined from the static pressure traverses taken along the length of the tubes as indicated in fig. 3 (a).

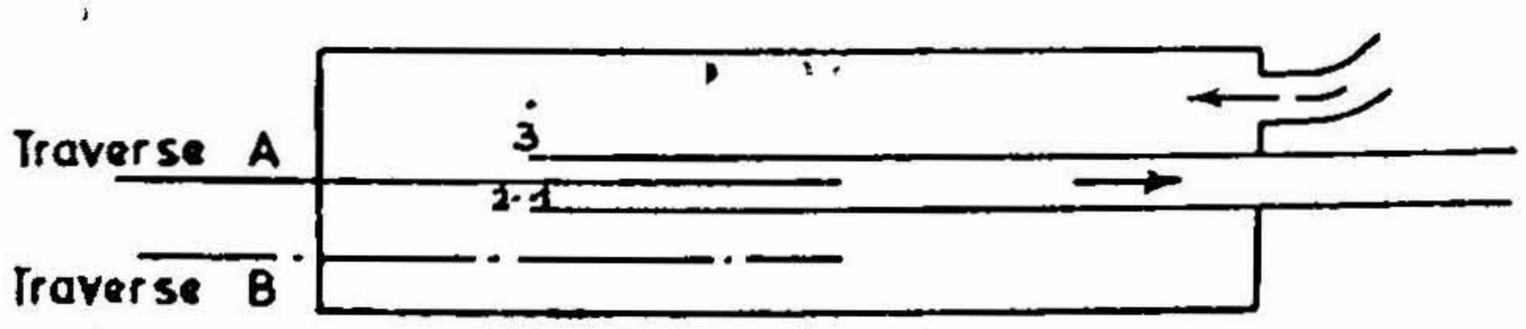

(a) Static pressure traverse for reversal-cum-contraction

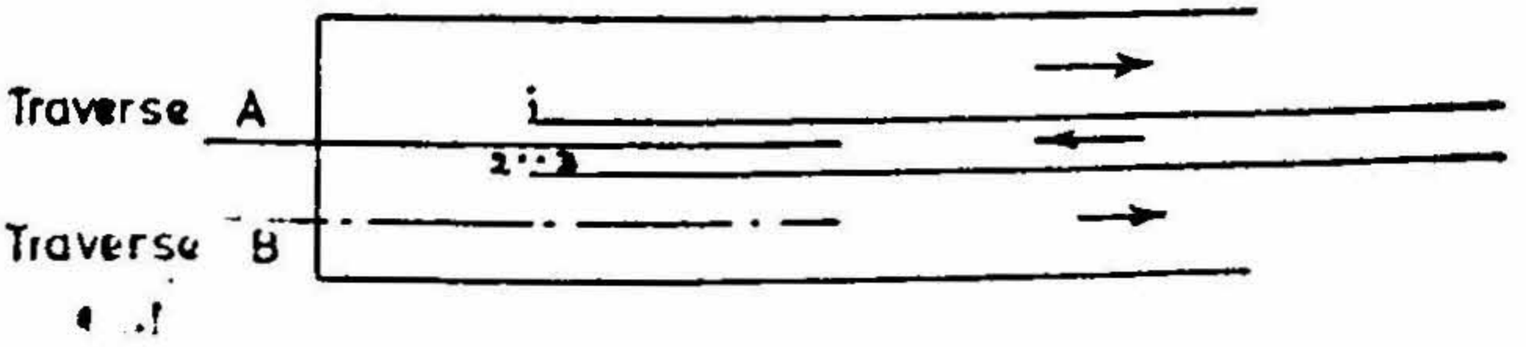

(b) Static pressure traverse for reversal-cum-expansion

FIG. 3. Static pressure traverse for flow reversing elements for evaluation of a_e and a_e.

A typical static pressure pattern is shown in fig. 4.

The calculated value of the head loss factor a_c is plotted against $1/N$ in fig. 5.

From fig. 5, it may be seen that for area ratios that are normally used in mufflers ($N < 0{\cdot}25$), the value of a_c would be nearly $1 - N/2$ as is the case for contraction

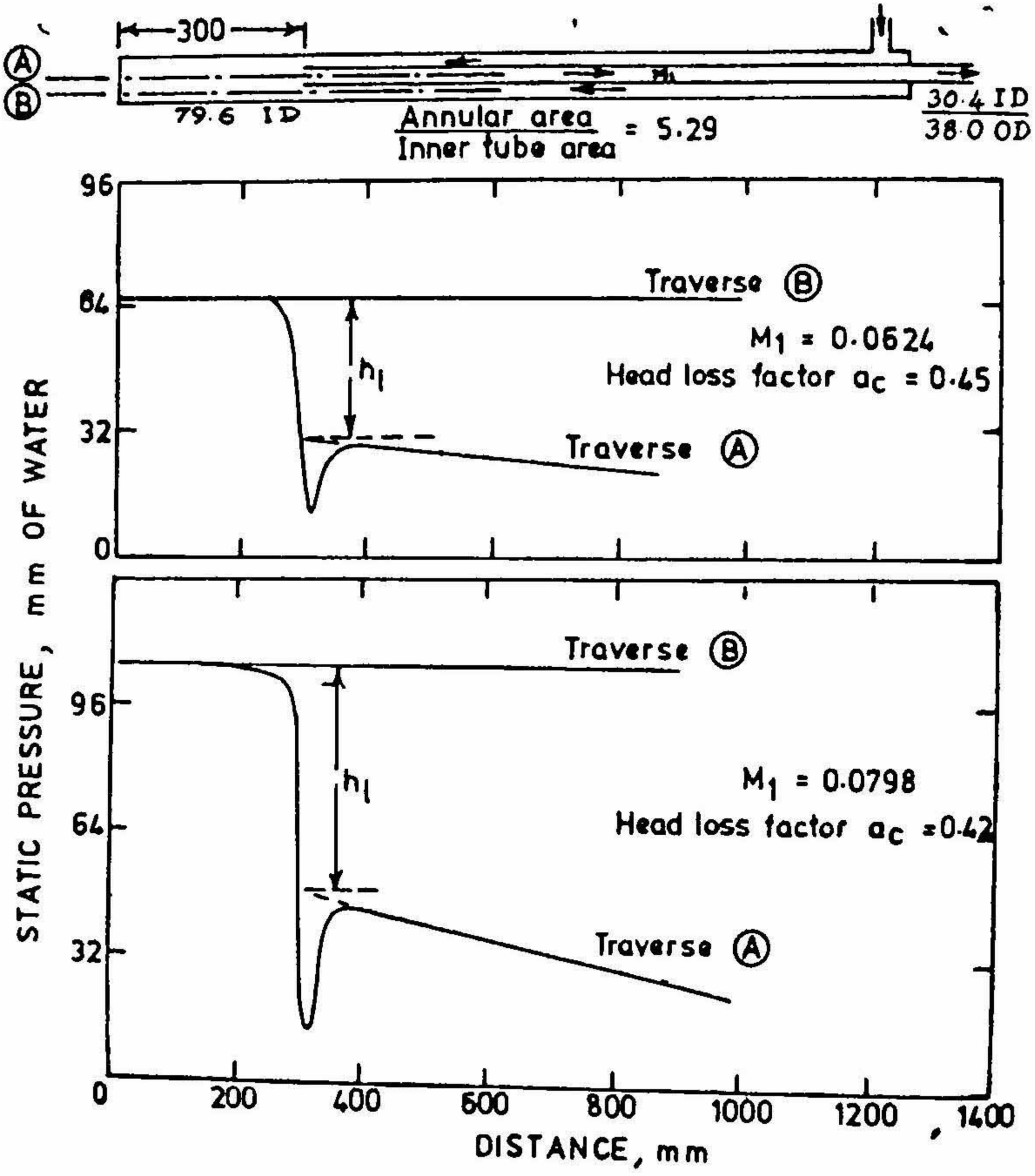

FIG. 4. Static pressure traverse for flow reversal-*cum*-contraction ($l_2 = 300$ mm).

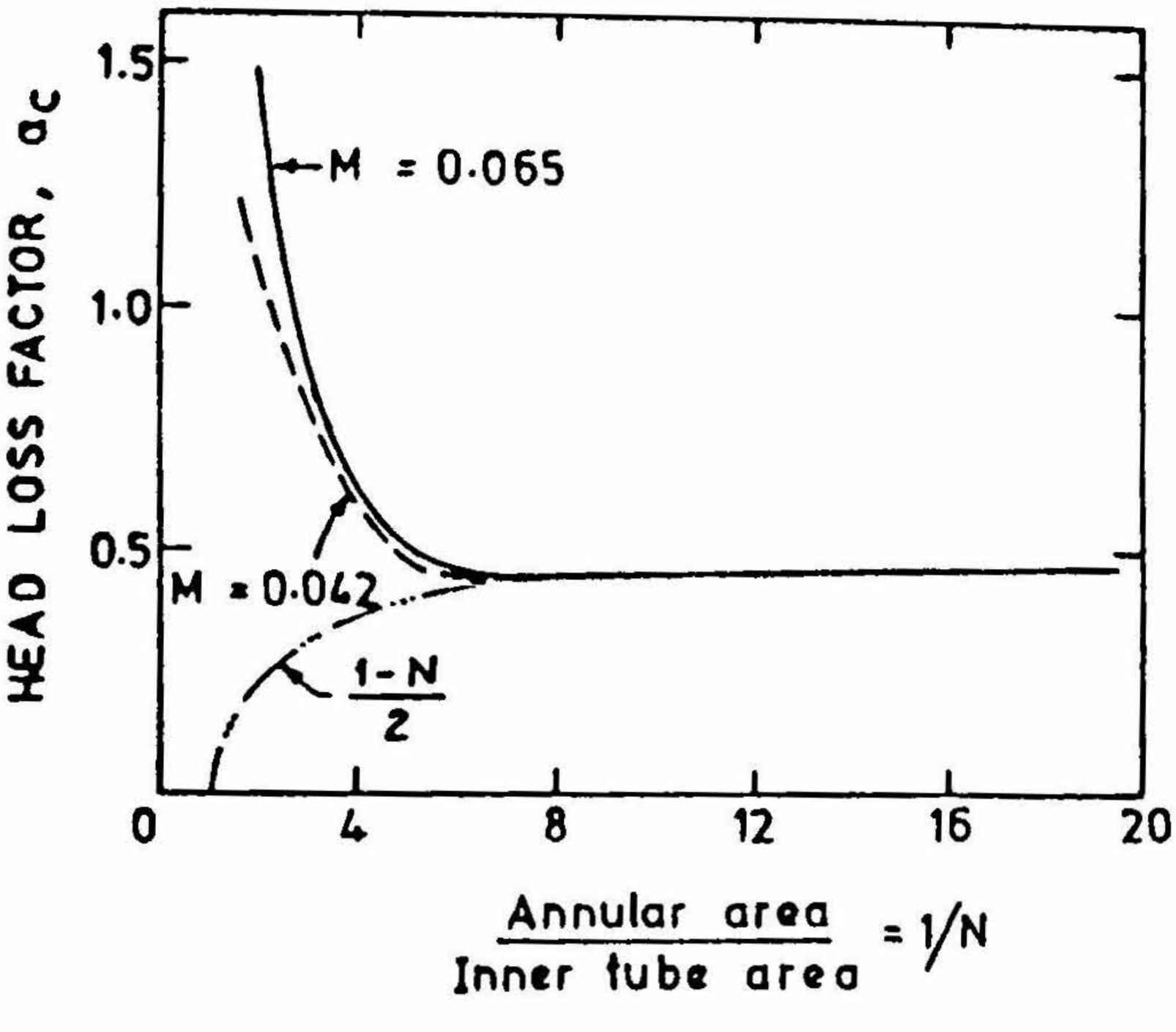

FIG. 5. Head loss factor for flow reversal-*cum*-contraction *vs* $1/N$; ——, $M = 0{\cdot}065$; - - - -, $M = 0{\cdot}042$; — ··· —, $(1 - N)/2$.

without reversal, and is more or less insensitive to the variation of flow Mach numbers normally found in exhaust mufflers. As should be expected, in the limiting case of a stationary medium ($M_1 = M_3 = 0$, $A = 0$), the matrix (19) reduces to

$$\begin{bmatrix} 1 & 0 \\ \frac{1}{Z_2} & 1 \end{bmatrix}. \tag{21}$$

3.2. *Flow reversal with expansion*

The transfer matrix for flow reversal-*cum*-expansion element can be derived with reference to fig. 2 (*b*) on the lines similar to that of reversal-*cum*-contraction.

The energy equations (6), (7) and (9) are valid for this case also while the conservation of energy equation (8) is to be modified as

$$p_{e,3} = p_{e,1} + a_e M_3 Y_3 v_{e,3} \tag{22}$$

where a_e is the head loss factor expressed as the ratio of the loss of total head across the reversal with expansion element to the dynamic head at the smaller tube.

Continuity equation is

$$v_{e,3} = v_{e,1} + v_2 + \frac{\delta M_1}{Y_1}. \tag{23}$$

Momentum equation gives

$$N(p_{e,3} + M_3 Y_3 v_{e,3}) + p_{e,1} + M_1 Y_1 v_{e,1} + \delta M_1^2 = N_{21} p_2 \tag{24}$$

where

$$N = \frac{S_3}{S_1} = \frac{Y_1}{Y_3} = \frac{M_1}{M_3} \tag{25}$$

$$N_{21} = \frac{S_2}{S_1} \tag{26}$$

$$v_2 = \frac{p_2}{Z_2} \tag{27}$$

and

$$Z_2 = -iY_2 \cot kl_2. \tag{28}$$

Solving eqns. (9), (22), (23), (24) and (27) simultaneously and assuming $M_1^2 \sim M_3^2 \ll 1$, (as is typical of automative exhaust mufflers) one gets the desired transfer matrix relation

$$\begin{bmatrix} p_{e,3} \\ v_{e,3} \end{bmatrix} = \frac{1}{N_{21} - AN(1+a_e)} \begin{bmatrix} N_{21} - A(N - a_e) & a_e M_3 Y_3 (N_{21} + AN^2) \\ 1+N & \\ Z_2 & N_{21} + AN^2 \end{bmatrix} \begin{bmatrix} p_{e,1} \\ v_{e,1} \end{bmatrix} \tag{29}$$

where

$$A = M_3 Y_3 Z_2.$$

If $NM \sim M^2 \sim N^2 \ll 1$, then $N_{21} \simeq 1 + N$ and the transfer matrix in eqn. (29) would reduce to

$$\frac{1}{1 + N - AN(1 + a_e)} \begin{bmatrix} 1 + N - A(N - a_e) & (1 + N) a_e M_3 Y_3 \\ 1 + N & \\ Z_2 & 1 + N \end{bmatrix}. \tag{30}$$

Experiments were conducted to evaluate the head loss factor a_e using static pressure traverse as indicated in fig. 3 (*b*), at different area ratios ranging from 1·9725 to 16·55 and flow Mach numbers up to 0·2076. A typical pressure pattern is shown in fig. 6.

The computed values of a_e are plotted against the mean Mach numbers of flow in the smaller tube in fig. 7.

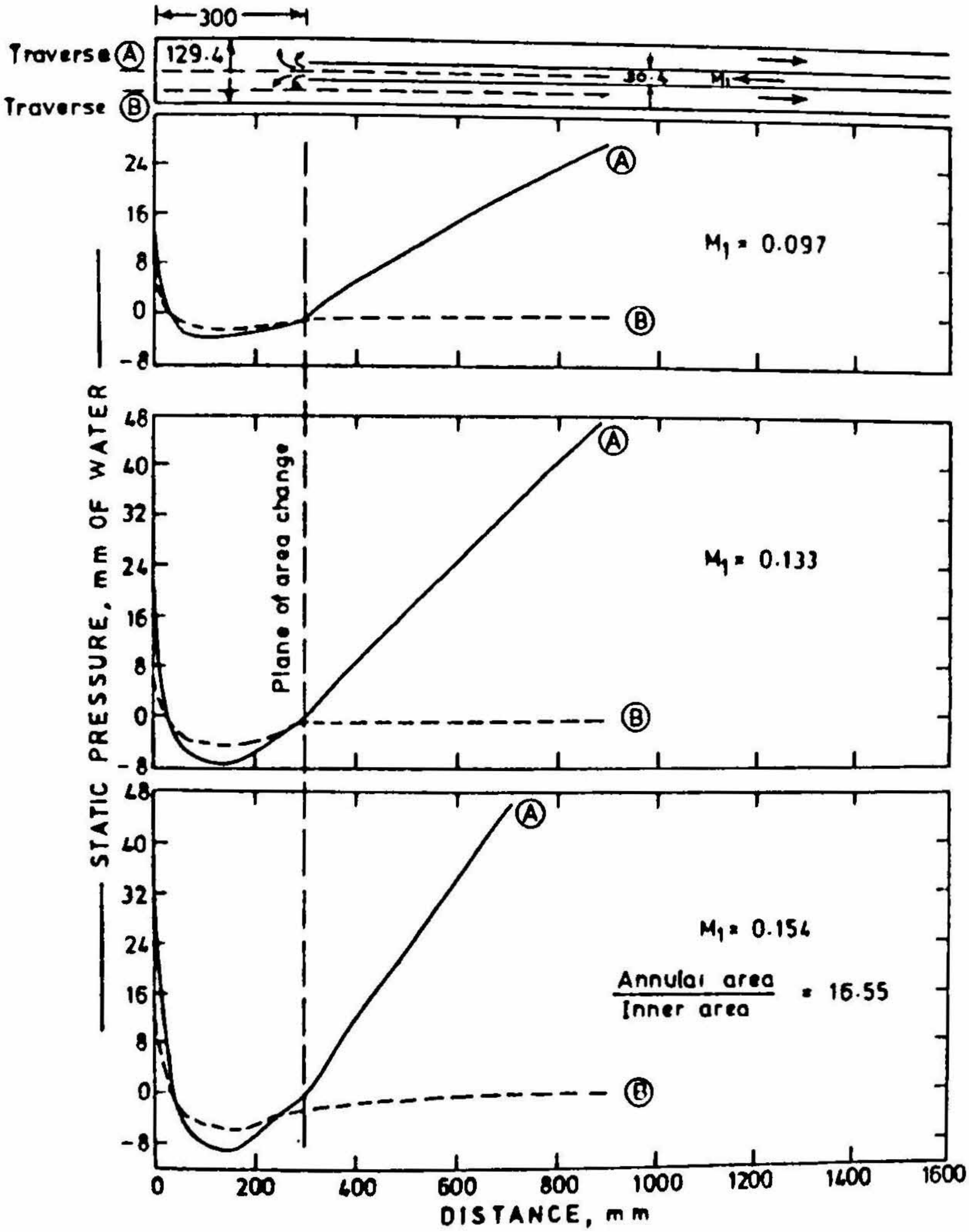

FIG. 6. Static pressure traverse for expansion-*cum*-flow reversal (l_2 = 300 mm).

It can be seen that the value of a_e is approximately unity as against the value between 2 and 3 suggested in refs. 6, 7.

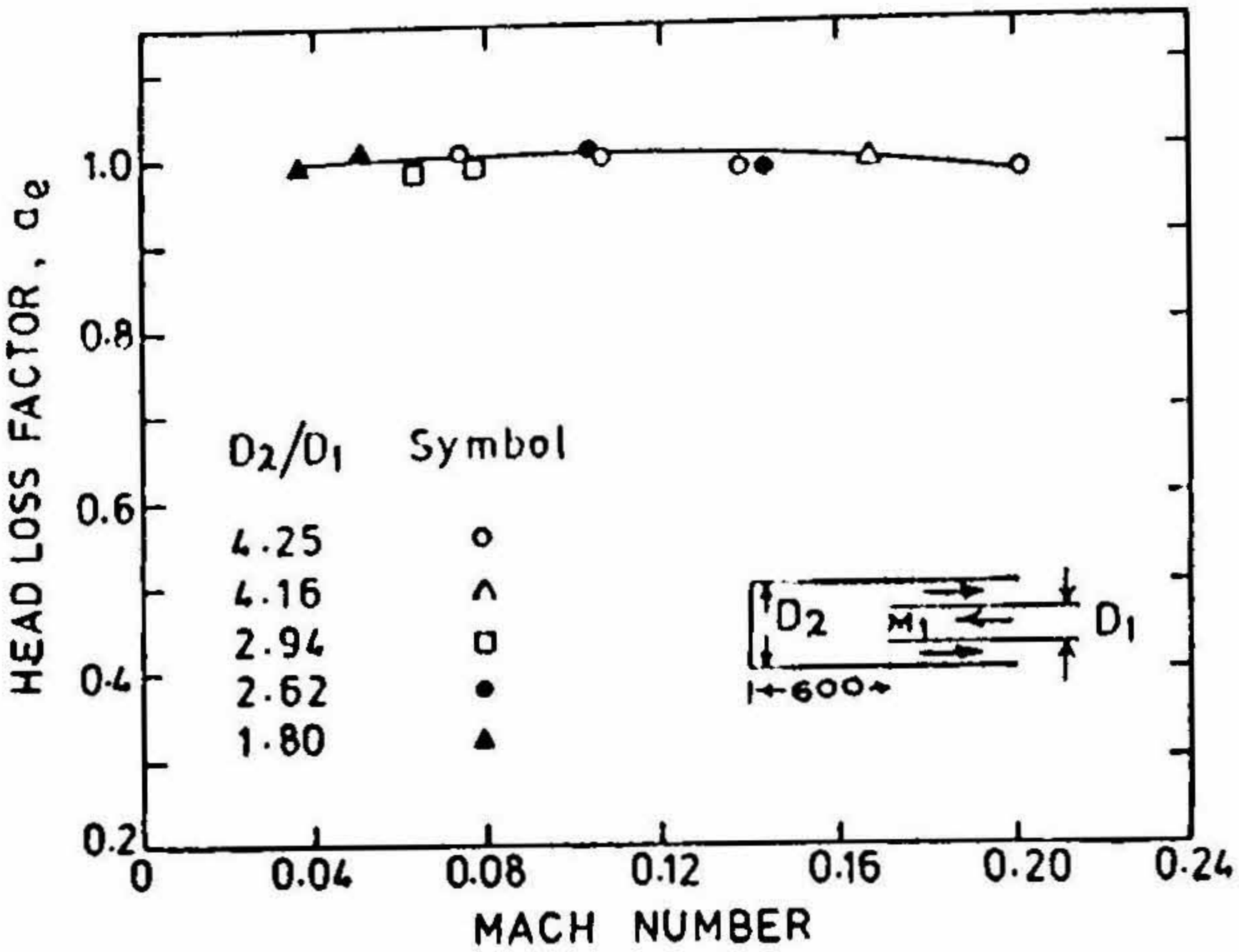

FIG. 7. Head loss factor for expansion-*cum*-flow reversal *vs* Mach number.

Comparing the transfer matrices (2) and (30), it is observed that the second column elements are modified by a factor $(1 + N)$. This would mean that $p_{e,1}$ in ref. 6 was slightly over estimated.

For a stationary medium, $A = 0$, $M_1 = M_3 = 0$ and hence, the transfer matrix would reduce to

$$\begin{bmatrix} 1 & 0 \\ 1 & 1 \\ Z_2 & \end{bmatrix} \tag{31}$$

as is expected.

4. Experimental verification

The validity of the transfer matrices derived above has been verified experimentally, though indirectly, by comparing the theoretical and experimental spectra of noise reduction across two experimental mufflers fabricated for this purpose. The dimensional details of the mufflers are shown in fig. 8.

Noise reduction was measured as the difference in sound pressure levels at two points marked 1 and 2, one near the exit end and the other upstream of the muffler with and without mean flow at a number of frequencies ranging from 90 Hz to 1250 Hz. The

lay-out of the experimental set-up is the same as that employed in ref. 9. Since the noise reduction with mean flow relates to the aeroacoustic pressures, a total pressure probe was used for the direct measurement of p_o. The noise reduction spectra are predicted theoretically for the muffler configurations (shown in fig. 8) by making

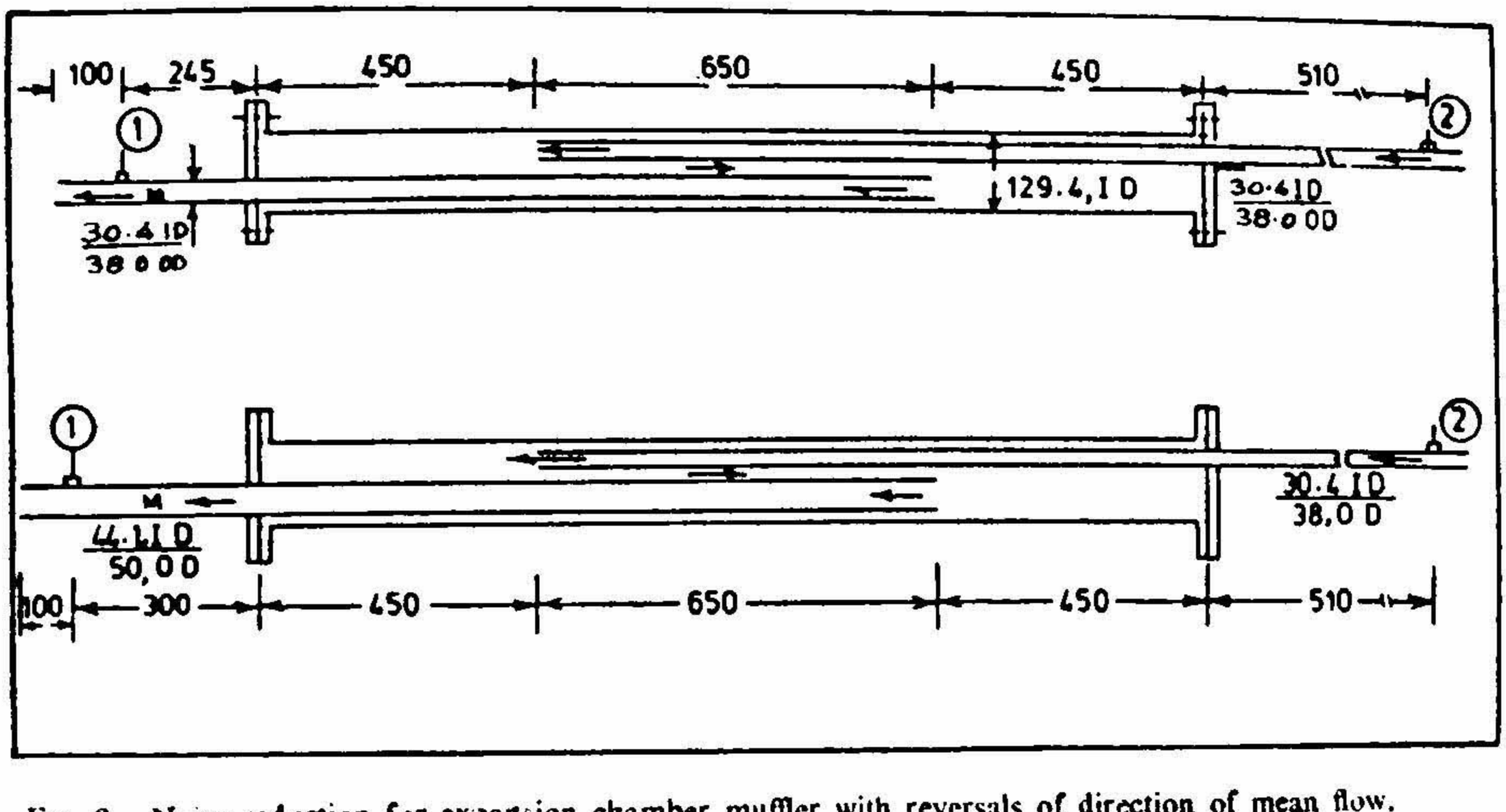

FIG. 8. Noise reduction for expansion chamber muffler with reversals of direction of mean flow.

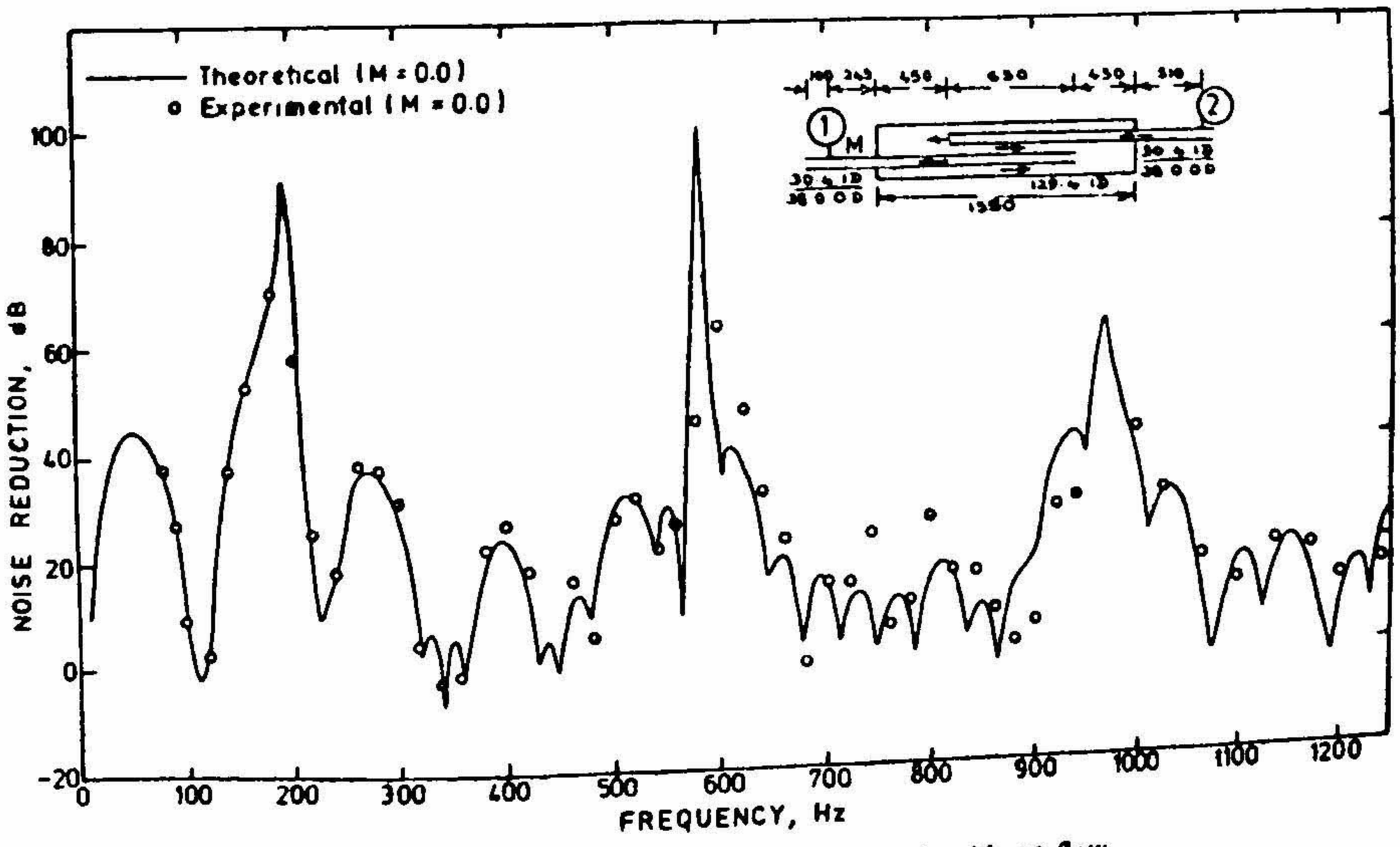

FIG. 9. Noise reduction characteristics of muffler with flow reversal, without flow.

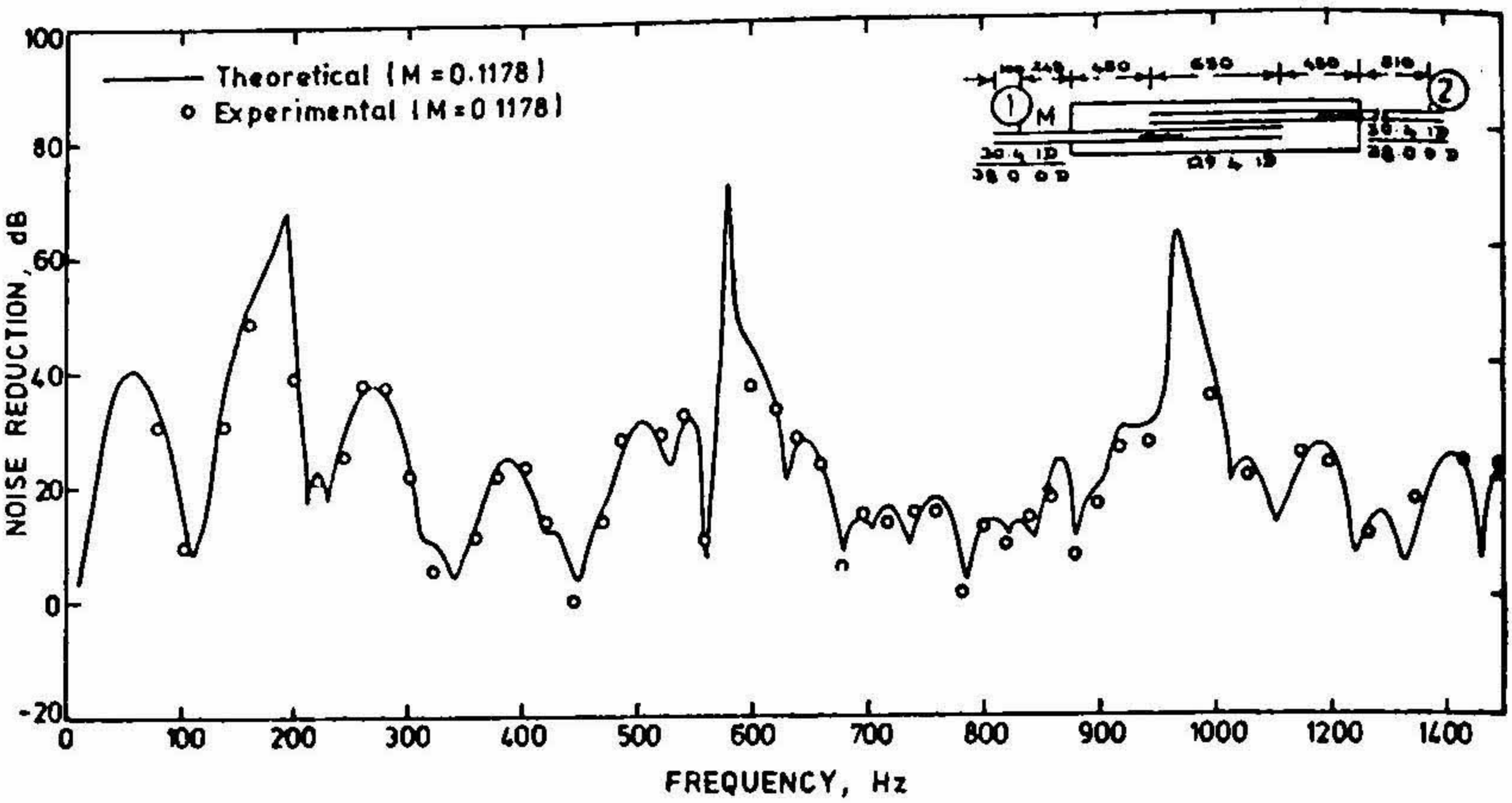

FIG. 10. Noise reduction characteristics of muffler with flow reversal, with mean flow.

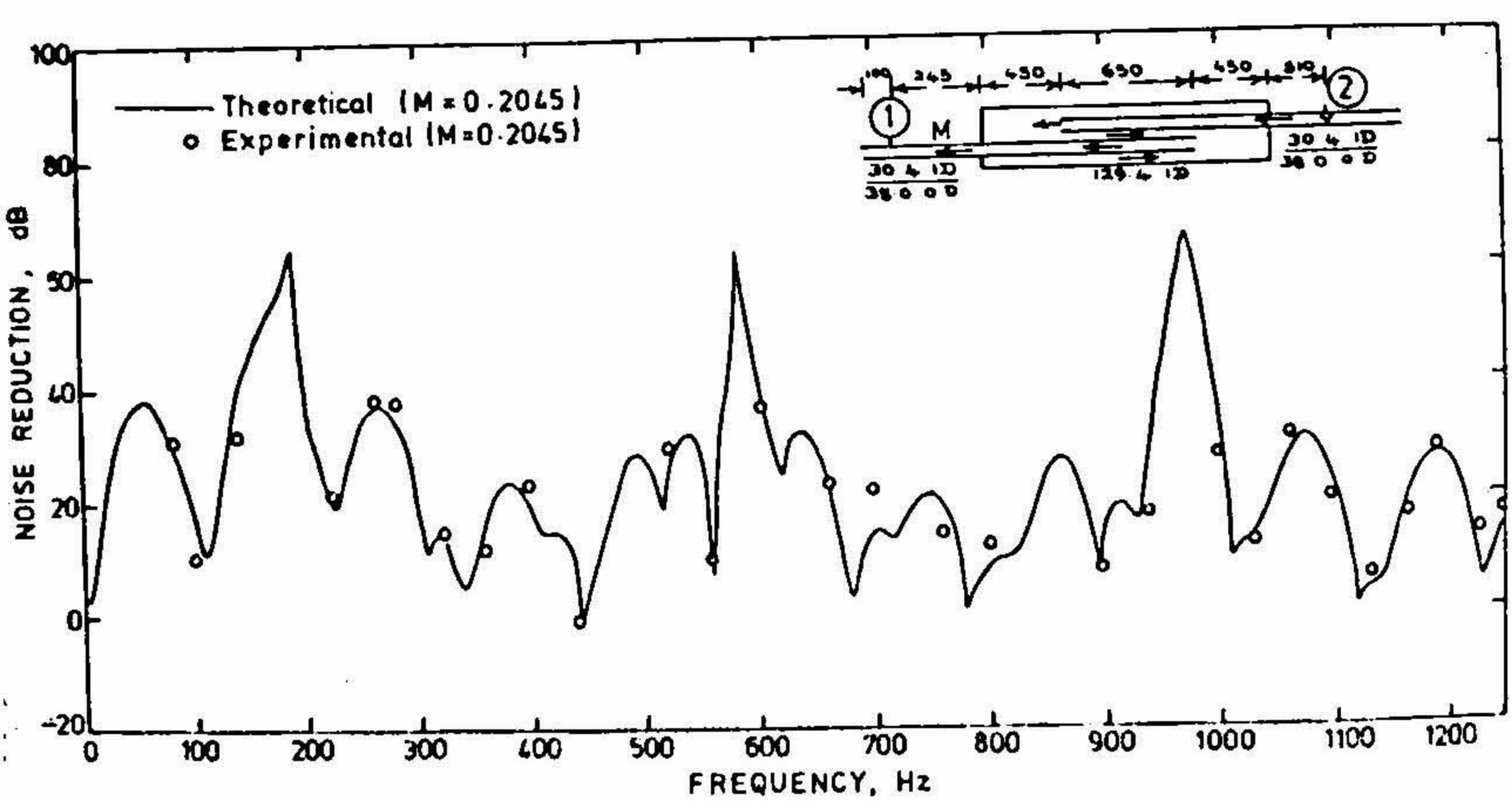

FIG. 11. Noise reduction characteristics of muffler with flow reversal, with mean flow.

use of the transfer matrices by means of a FORTRAN program which takes into account the radiation impedance and tube attenuation constant as modified by the convective and dissipative effects of mean flow, and are plotted in figs. 9 to 13 for different Mach numbers of mean flow. The measured values of noise reduction are indicated in the respective plots.

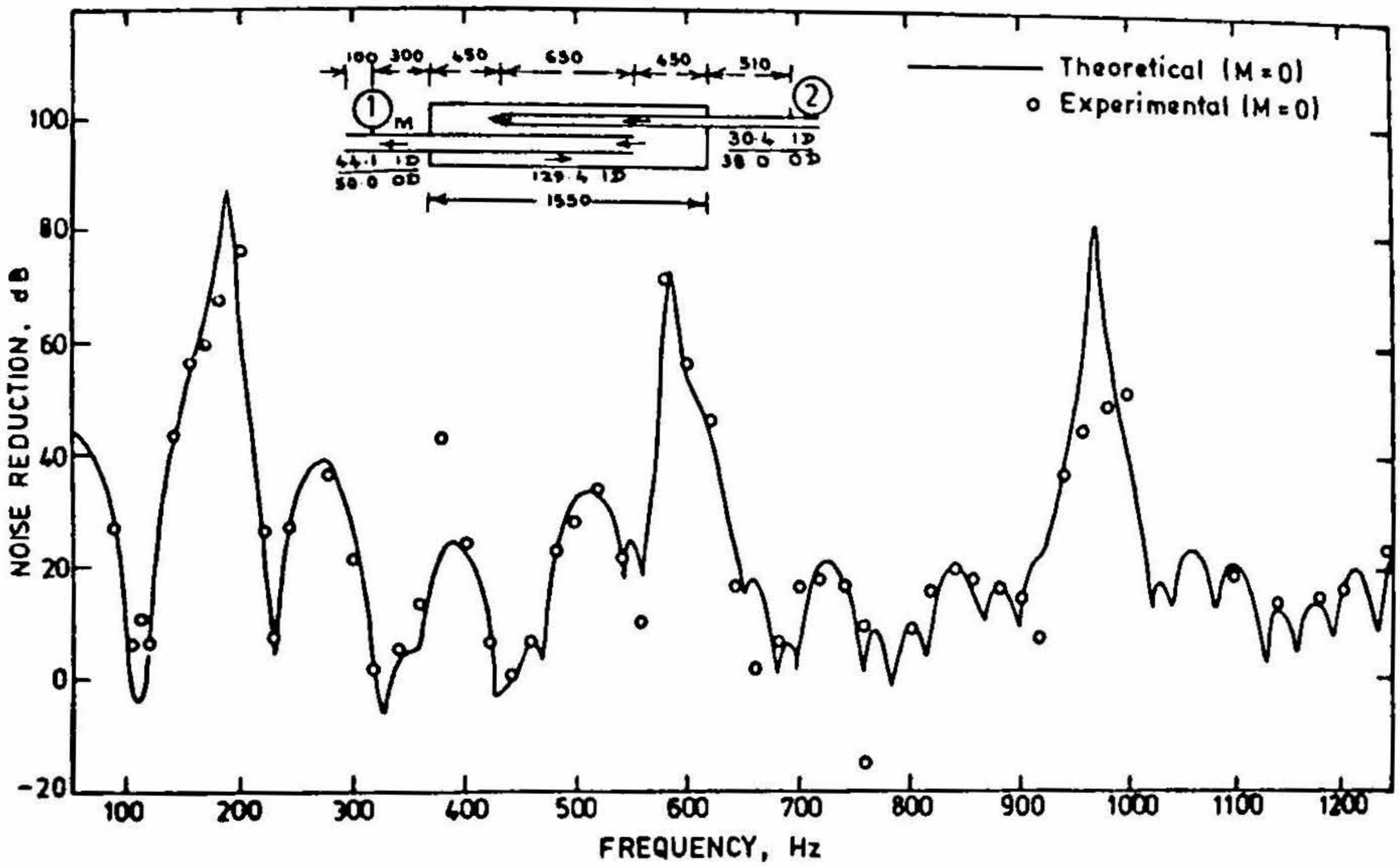

FIG. 12. Noise reduction characteristics of muffler with flow reversal, without flow.

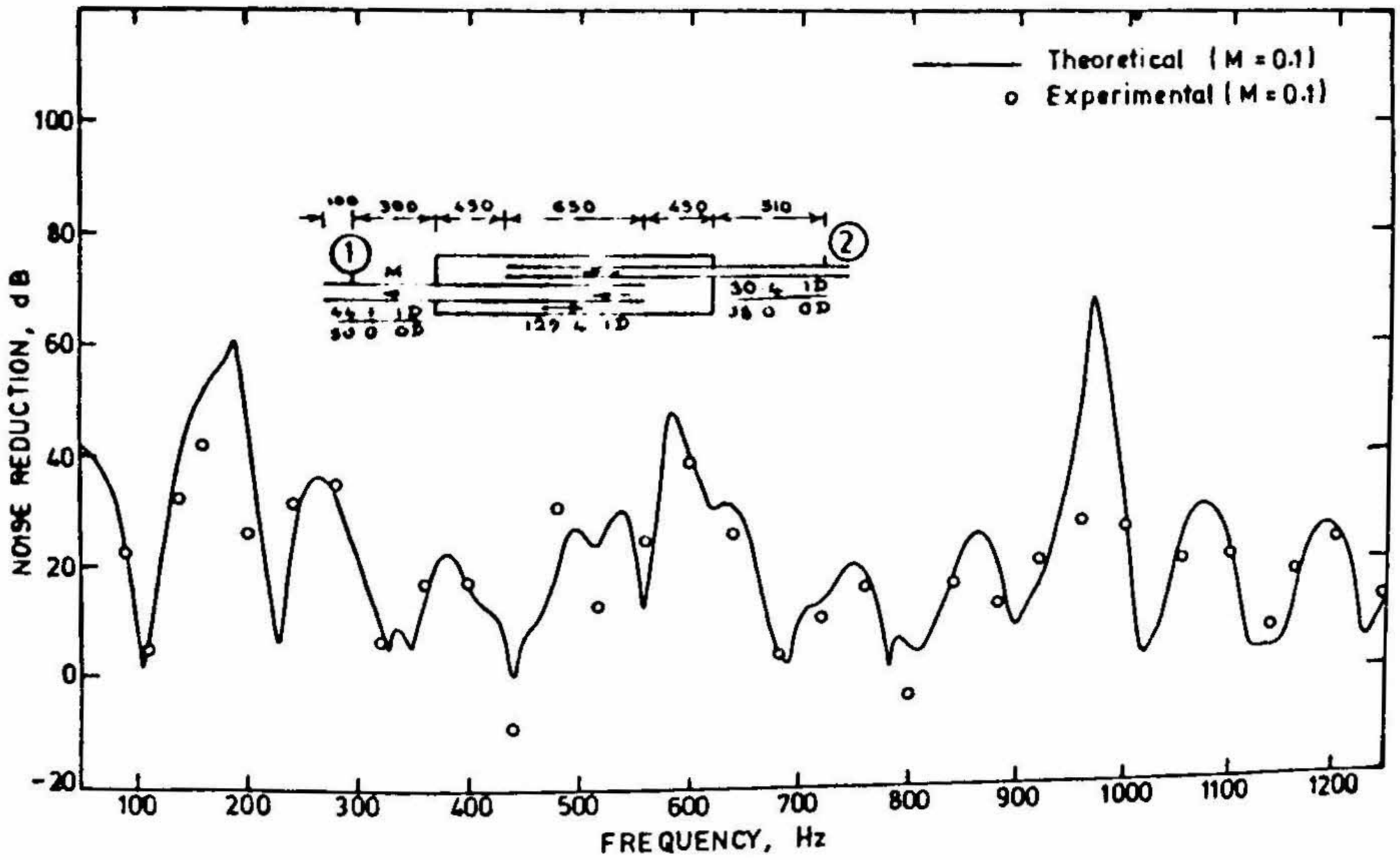

FIG. 13. Noise reduction characteristics of muffler with flow reversal, with flow.

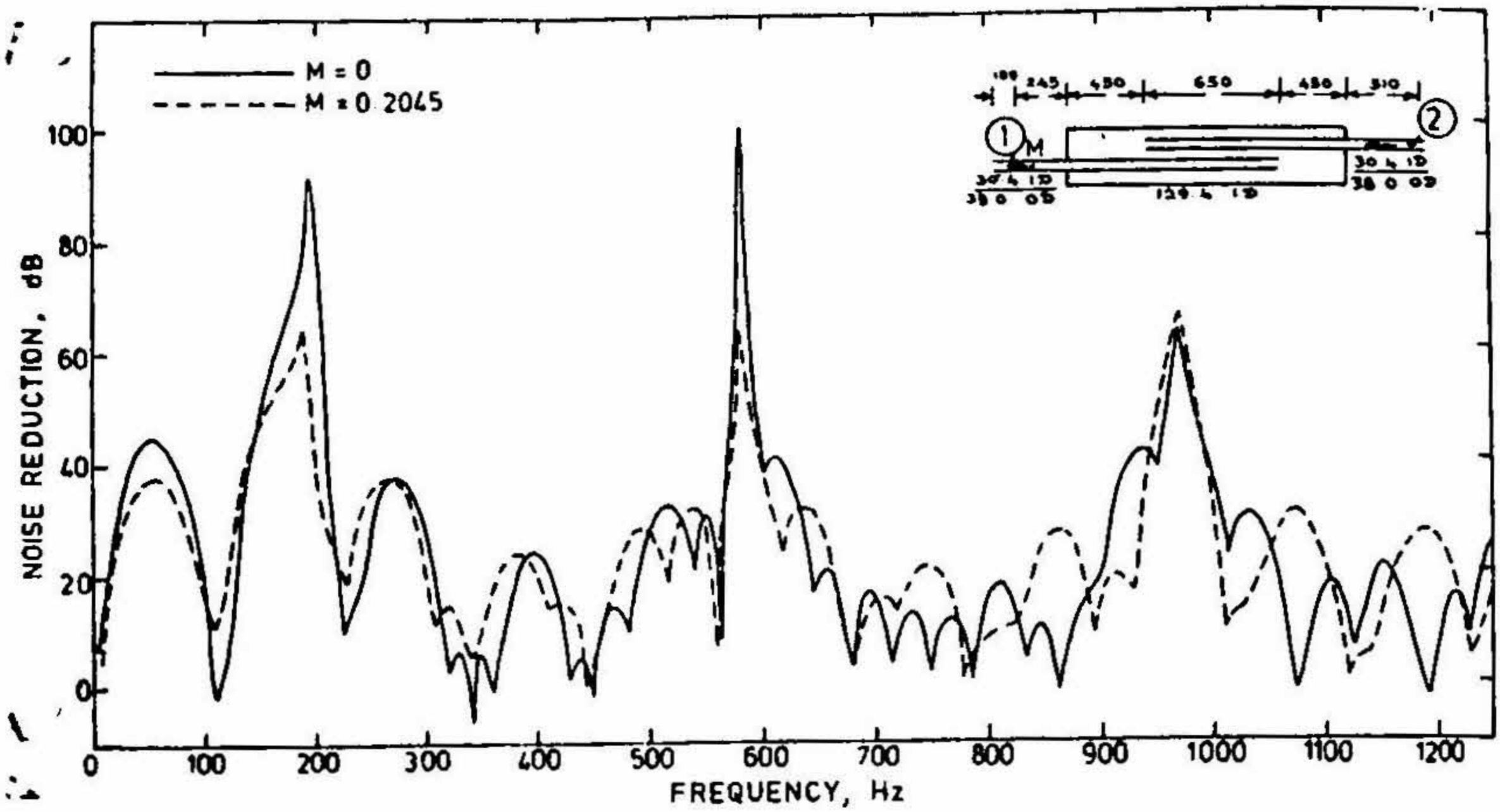

FIG. 14. Effect of mean flow on noise reduction characteristics of muffler with flow reversal.

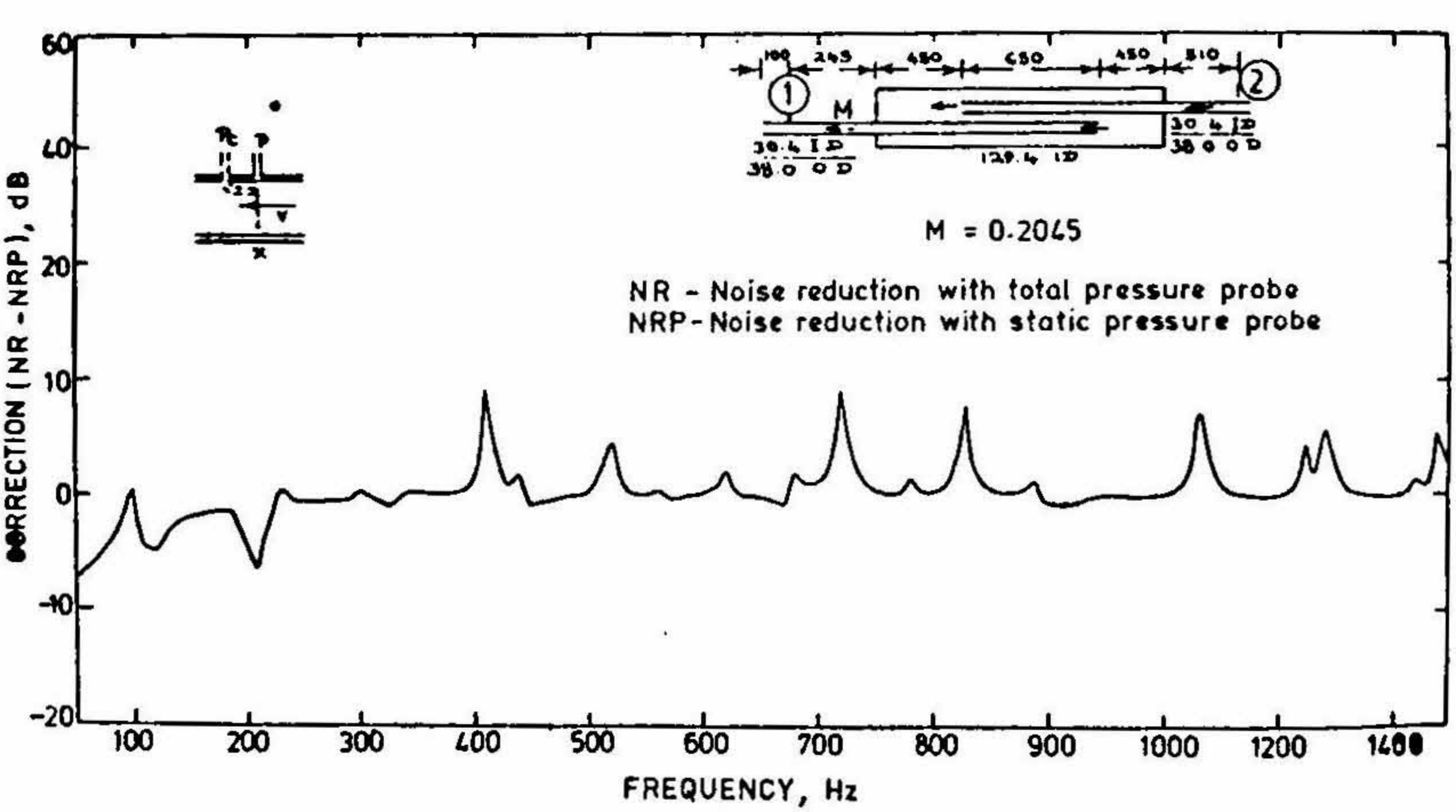

FIG. 15. Correction in noise reduction (NR–NR′) *vs* frequency for a muffler with flow reversal.

Figure 14 shows the effect of flow on the theoretical noise reduction spectrum. If wall static pressures are measured instead of the aeroacoustic pressures, the calculated values of noise reduction would be in error. The probable error in the theoretical

noise reduction predicted if sound pressure levels were measured by wall static pressure probe, is shown in fig. 15. The scheme of calculation of error is given in Appendix of ref. 9.

The results indicate the following:

1. Experimental values of noise reduction are in good agreement with the results predicted by the use of the transfer matrices, thereby confirming the validity of the transfer matrices.

2. The three-dimensional effects become predominant only at higher frequencies, which are very much lower than the classical cut-off values for reasons explained in ref. 9.

3. The error involved in the noise reduction if SPLs are measured by wall static-pressure probe instead of a total-pressure probe, would generally be small (of the order of 0·2 *dB*) except at resonance frequencies where the error would be higher depending on the flow Mach numbers as shown in fig. 15.

4. The effect of mean flow on the noise reduction spectrum is to flatten out the resonance peaks and troughs with slight shift in the resonance frequencies. This is evident from fig. 14. Measurements of SPL at frequencies corresponding to the peaks of noise reduction curves were difficult and unreliable as the SPL at the downstream station was below the ambient noise level due to flow turbulence.

5. Conclusions

The present theoretical analysis brings about a number of improvements in the transfer matrices of flow reversing elements suggested by earlier investigators[6, 7]. In particular,

(i) the effect of tube wall thickness in the formulation has been taken into consideration in eqns. (18) and (29).

(ii) the head loss factors for the reversal elements with contraction and expansion have been estimated experimentally as $1 - N/2$ and 1·0 respectively. This eliminates the previous assumptions of zero and 2 to 3 respectively[6, 7].

(iii) the scheme of derivation of the transfer matrices now suggested makes the analysis of reversed flow mufflers simpler and conceptually more tractable.

The changes incorporated into the transfer matrices make only a marginal difference up to 1*dB* in the noise reduction except at peaks and troughs where it is substantial (up to 5 *dB*) for a muffler with only one flow reversing chamber. For commercial mufflers employing 2 to 3 chambers the difference would be considerable.

Acknowledgements

The work forms part of the doctoral work 'Some studies on the prediction and verification of the aeroacoustic performance of exhaust mufflers" by the first author at the Indian Institute of Science, Bangalore, India. The authors gratefully acknowledge the facilities provided by the Institute and the financial assistance extended by the Lal Bahadur Sastri Technological Research Centre, Government of Kerala.

References

1. CROCKER, M. J. — *Internal combustion engine exhuast muffling*, NOISE-CON-77, NASA Langely Research Center, 1977, pp. 331–352.

2. SULLIVAN, J. W. AND CROCKER, M. J. — Analysis of concentric tube resonators having unpartitioned cavities, *J. Acoust. Soc. Am.*, 1978, 64 (1), 207–215.

3. SULLIVAN, J. W. — A method for modelling perforated tube muffler components. I. Theory, *J. Acoust. Soc. Am.*, 1979, 66 (3), 772–778.

4. SULLIVAN, J. W. — A method for modelling perforated tube muffler components. II. Applications, *J. Acoust. Soc. Am.*, 1979, 66 (3), 779–788.

5. MUNJAL, M. L. — Velocity ratio-*cum*-transfer matrix method for evaluation of a muffler with mean flow, *J. Sound Vibr.*, 1975, 39 (1), 105–119.

6. MUNJAL, M. L. AND BAPAT, U. B. — Aeroacoustic analysis of certain branch resonators, 1977. *Proc. Conf. Mech. Engrs. Delhi*, Dec. 1977, T.D. 1–24.

7. THAWANI, P. T. — *Analytical and experimental investigation of the performance of exhaust mufflers with flow*, Ph.D. Thesis, 1978, University of Calgary.

8. MUNGUR, P. AND GLADWELL, G. M. — Acoustic wave propagation in a sheared fluid contained in a duct, *J. Sound Vibr.*, 1969, 9, 28–48.

9. PANICKER, V. B. AND MUNJAL, M. L. — Aeroacoustic analysis of mufflers with simple and extended tube expansion chambers, *J. Indian Inst. Sci.*, 1981, 63 (A), 1–19.